J Solid State Electrochem (2008) 12:1085–1091
DOI 10.1007/s10008-007-0440-z

ORIGINAL PAPER

Pd electrodeposited from membrane-separated thin layer cell

Anna Frydrychewicz · Aleksander T. Bieguński · Krystyna Jackowska · Galina A. Tsirlina

Received: 11 July 2007 / Accepted: 30 September 2007 / Published online: 7 November 2007

Abstract Polycarbonate (PC) membranes of different porosity (from 50 nm to 400 nm pore size) were used as separators in a thin layer cell for palladium electrodeposition. Atomic force microscopy (AFM) confirmed the formation of Pd layer between the cathode and porous membrane, with subsequent growth inside the pores induced by space limitations of further growth of initial layer. Our estimates confirm that at this stage Pd deposit feels the pronounced mechanical pressure and consider it as a possible reason of specific hydrogen sorption behaviour in the region of β-phase hydride formation. Up to c.a. 1.0 H/Pd atomic ratio is observed for some samples. We consider possible (nano)structural peculiarities responsible for this behaviour.

Keywords Hydrogen sorption · Membrane assisted synthesis · Palladium nanostructures · Palladium thin layers

Introduction

The most typical approach to templating with porous membranes is providing the space limitations for the deposit growth inside the pores. However it is not the unique possibility to affect the deposit properties: membranes can be also used in thin-layer deposition cell as separators between two parallel plates. This configuration gives a chance to obtain less dendric and mechanically stable materials than in thin layer cells without electrode separation used for fabrication of fractal deposits [1]. To illustrate this approach we report below Pd electrodeposition. Our choice of Pd results from its unique ability to absorb and store hydrogen [2]. Hydrogen solubility and diffusion reported earlier for Pd electrodeposited under various modes [3–17] demonstrate the pronounced difference from hydrogen sorption by metallurgical Pd. Dispersed Pd nanostructure (particle size, grain boundaries, lattice defectiveness and compression) responsible for its specific behaviour is controlled by preparation technique. In particular template or quasi-template assisted deposition [9, 15, 16] is already recognized as the effective instrument for nanostructuring.

Pd deposition from chloride bath always results in formation of nm-size coalesced crystals. In usual cell configuration [3, 4] Pd deposition can be affected by deposition potential. The latter is responsible for the ratio of primary/secondary nucleation-growth rates and by these means for formation of intergrain boundaries and lattice compression. We would like to demonstrate that nano-structural features of electrodeposited Pd can also be affected by mechanical pressure appearing in a very simple configuration of membrane-separated two electrode cell. The preliminary experiments confirmed that the initial deposition starts in a gap between cathode and membrane and results in formation of Pd layer outside pores. Starting from some moment the deposit is already observed inside the pores, manifesting the pronounced limitations of further mechanical pressing of PC membrane, with its rather high Young modulus [18]. We report below some observations related to the effect of this pressure induced by metal growth on hydrogen absorption properties of Pd deposits.

A. Frydrychewicz · A. T. Bieguński · K. Jackowska (✉)
Laboratory of Electrochemistry, Chemistry Department,
Warsaw University,
Pasteur 1,
02-093 Warsaw, Poland
e-mail: kryjacko@chem.uw.edu.pl

G. A. Tsirlina
Department of Electrochemistry, Moscow State University,
119992 Moscow, Russia

Materials and methods

Palladium structure formation

Pd samples were fabricated on templates in electrochemical dual electrode sandwich system containing porous polycarbonate (PC) membrane. A sandwich system consisted of two ITO (indium tin oxide coated glass) slides separated by solution filled membrane (Fig. 1). The upper slide operated as a working electrode (WE), while the bottom one was used as the counter and reference electrode simultaneously (CE/RE).

Before deposition, the ITO slides were washed with acetone and placed in an acetone sonic bath for 20 min. Later they were rinsed with distilled water and dried. The deposition bath contained 2.5 M $PdCl_2$ in 5 M HCl. First, a larger ITO slide (2×4 cm) (RE/ CE) was covered with a dry membrane (2.5 cm in diameter). Next, a drop (c.a. 0.5 ml) of deposition solution was placed on top of the membrane. After the solution spread and soaked the membrane the second slide (1×4 cm) (WE) would be placed over the membrane and pressed on. The amount of the solution applied to the membrane was large enough to ensure electrical contact between the slides. When the smaller amount was used, no stable deposition response was ever obtained. Deposition current transients were not exactly reproducible, demonstrating two general types of behaviour (slow decrease of current or typical nucleation maximum). We assume that the reason of low reproducibility is hardly controllable residual filling of membrane pores with air. At this stage we do not consider this problem as something crucial because we do not study nanowires formed inside the pores: major portion of Pd in our samples is formed in the gap.

Slides were pressed tightly together with a clip, the working slide would be placed on top so that the amount of excess liquid leaking to the space between the ITO cathode and membrane would be minimized.

When potential step (from 0.0 to-0.5 V) was applied to WE, palladium started to deposit onto ITO slide from solution containing in a thin layer and inside the membrane pores. The deposition periods t_{dep} were 150, 350 and 500 s long. The charges spent in all deposition experiments corresponded to negligible total consumption of Pd(II), so bath composition was never changed in the course of deposition. After deposition, the membrane was carefully peeled off the WE ITO slide. The WE slide was than rinsed with distilled water to remove all traces of the deposition solution.

At this stage we failed to work out the procedure to delete the membrane without affecting the amount of deposited palladium. To estimate palladium loading in a given sample, Pd subjected to voltammetric experiments was later dissolved electrochemically in 1M HCl by applying the potential scan from-0.2 V towards more positive potentials at 20 mVs^{-1}, to obtain the anodic peak of palladium oxidation. The amount of palladium in the sample was calculated from the total charge corresponding to this peak. For samples under study Pd loadings ranging from 0.4 to 2.1 nanomole were found.

Voltammetric experiments and electrochemical hydrogen loading of Pd structures were carried out in 1 M $HClO_4$ solution in non-separated conventional three electrode cell. The working electrode was the ITO slide with Pd deposit, as for the counter and reference electrodes Pt gauze and Ag/AgCl(0.1 M KCl) were used respectively. All potentials are given in respect to that reference electrode. Prior to each electrochemical experiment the solution was deaerated for 10 min with Argon gas.

Hydrogen absorption behaviour of deposits was examined using the anodic hydrogen extraction (see [17] for details). The electrodes were charged in 1 M $HClO_4$ for 100 s at different sorption potentials E_s (from-0.12 to-0.28 V, i.e. from 0.17 to 0.01 V vs RHE). After this sorption period, the potential was scanned to + 0.7 V and the anodic peaks were integrated. Charge was recalculated to H/Pd atomic ratio.

Membranes, chemicals and apparatus

All chemicals (HCl, $PdCl_2$ and $HClO_4$) purchased from Merck were of analitycal grade and used as received, water was triply distilled with milipore.

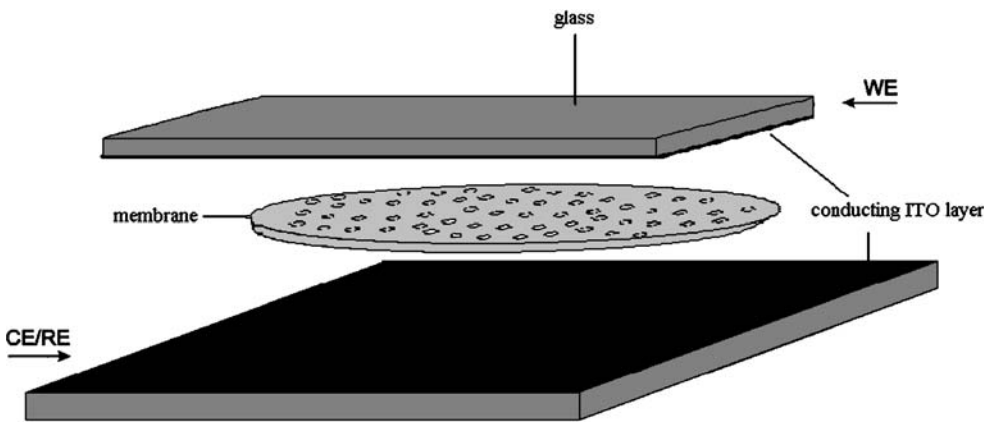

Fig. 1 A sandwich cell separated by PC membrane

Nucleopore Polycarbonate membranes of 100, 200, 400 and 50 nm pore diameter were purchased from Whatman. Membrane thickness was 20 μm, and rated pore densities ranged between 1.5 and $6*10^8$ pores cm^{-2}.

Electrochemical experiments were performed on Autolab EcoChemie equipped with GPES 4.9 and connected to IBM computer. AFM images were recorded on Nanoscope IIIA, Digital Instruments.

Results and discussion

AFM and cyclic voltammetry

AFM images (Fig. 2) show the globular structure of Pd layer. Typically the size of globulas is 80–120 nm, when the size of initial reference fragments of bare ITO is close to 30 nm (not shown in the Figure). The membrane pore diameter (compare A, D, and E images) and deposition time (compare A, B, and C images) affect the size and shape of the separate fragments on top of this layer. Basically they look like rings or islands, and the diameters are close to pore size.

For 400 nm membrane and 350 s deposition time, the predominating on top fragments are rings of c.a 360 nm diameter (Fig. 2, image a). For shorter deposition time 150 s, the rings are less complete (Fig. 2, image b). Observations agree with the assumption that starting from some moment palladium nucleates in the vicinity of the pore walls and then the deposit expands vertically. A possible reason of near-wall nucleation is the presence of gas bubbles inside the pores. Note that the distance between two neighbouring rings in Fig. 1 a, b is close to the distance between the centers of two neighboring pores. However we observe no periodic structure. We can not exclude that many pores are completely blocked by gas bubbles, especially if being of smaller diameter.

Rare cone-like islands instead of rings were observed after longer deposition time (Fig. 2, image c). Their shape differs from the typical shape of ITO globulas and Pd underlayer.

In the case of 200 and 100 nm membranes and 350 s deposition time the predominant form of palladium fragments growing inside the pores is conic nanoisland of diameter close to the pore size (Fig. 2, images d and e). Again, only rare pores start to be filled. However this ‘occasional’ growth indicate that the layer between cathode and membrane already meets some mechanical resistance of compressed membrane. This moment is determined mainly by deposition time, as for one and the same deposition time, the thickness of initially grown layer is

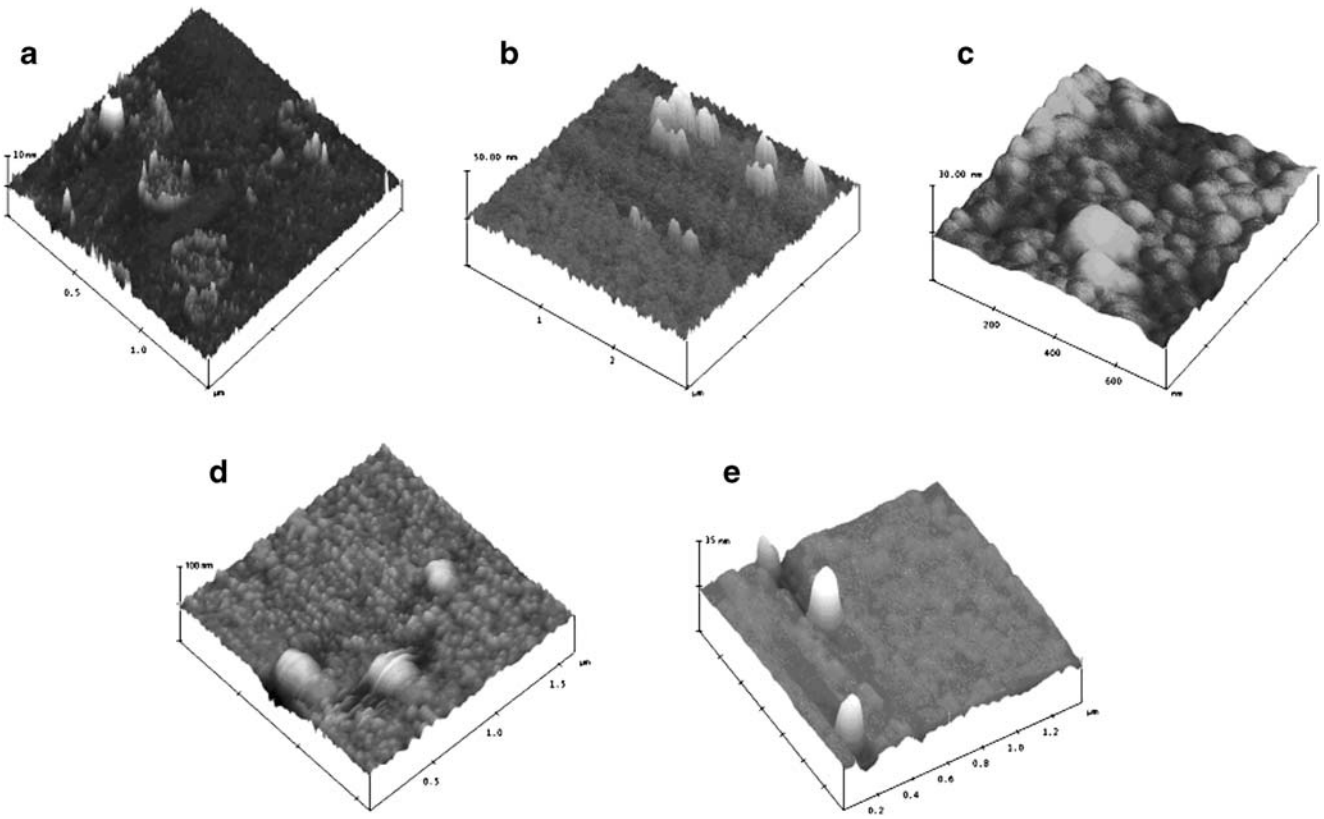

Fig. 2 AFM images of ITO\(Pd nanostructure) electrodes obtained with the use of different membrane templates and at different deposition times t_{dep}: (**a**) 400 nm membrane, t_{dep}=350 s, (**b**) 400 nm membrane, t_{dep}=150 s, (**c**) 400 nm membrane, t_{dep}=500 s, (**d**)200 nm membrane, t_{dep}=350 s, (**e**) 100 nm membrane, t_{dep}=350 s

responsible for this critical moment. From deposition charge one can roughly estimate this thickness as c.a. 10–30 nm. This means that the original thickness (L) of the membrane changes by c.a. 0.1%. Corresponding pressure can be estimated from the formula:

$$P = E(\Delta L/L)$$

, where E is Young modulus equal 2.2 GPa for polycarbonate [18]. Within the accuracy of ΔL estimate one can conclude that the pressure affecting Pd growth is 10–30 times higher than atmospheric pressure. These extremely rough estimates should be surely detailed taking into account the external clipping action. However there are no doubts that the excess pressure is rather high for already very thin deposits.

After palladium template deposition and membrane removal all the samples were examined by cyclic voltammetry. First, CV curves (20 mV s^{-1}) were recorded in 1 M $HClO_4$ solution in -0.2 to 1.2 V interval. A typical oxygen adsorption region was observed, with the pronounced contribution of Pd deposition currents. Lower charge (as compared to anodic branch) was found in the region of cathodic oxygen desorption, and just these desorption peaks were integrated to estimate the true surface area of Pd deposits. The charge value for 1 cm^2 of true surface area was assumed to be 0.42 mC.

For the majority of deposits 20–25 m^2g^{-1} specific surface areas were obtained after normalizing to the total amount of Pd determined in the final experiment. Slightly lower value of c.a. 15 m^2g^{-1} was found for the thinnest deposit (t_{dep}= 150 s) assumed to grow under smaller pressure. Let us stress that if oxygen monolayer is incomplete the experimental value of charge corresponds to even higher surface areas.

These values of the specific surface areas are substantially higher than the usual values for electrodeposited Pd consisting of 5–10 nm crystals (1–10 m^2g^{-1}) [3, 4, 8, 9]. Correspondingly, the sizes of crystals in our samples are similar or even smaller (if crystals are more coalesced). This means that the globules imaged in Fig. 2. are surely complex fragments consisting of nanocrystals.

To conclude this section, we deposited nanograined palladium material under mechanical pressure continously increasing in the course of deposition. This is still the hypothesis based on semi qualitative analysis and approximate estimates. In the next section we are looking for correlation of pressure appearing in the course of deposition and hydrogen sorption properties of electrodeposited Pd.

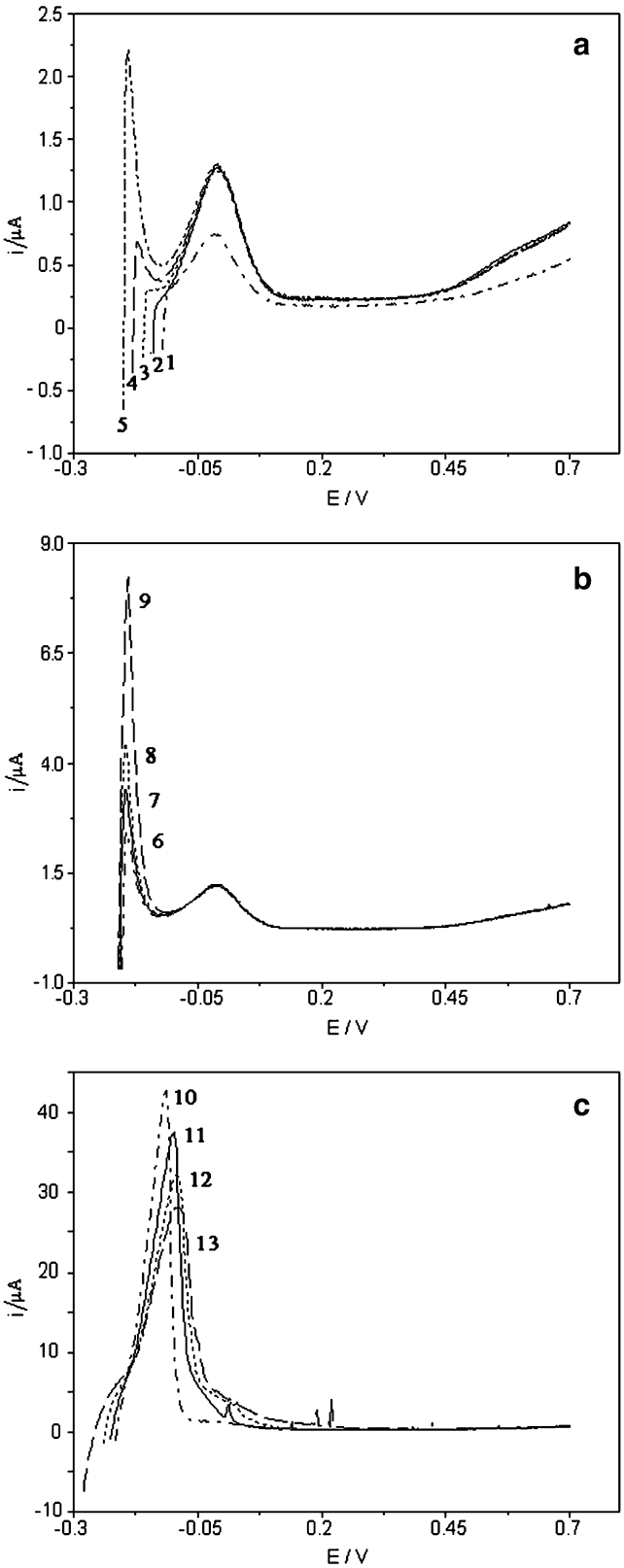

Fig. 3 The i~E curves of ITO\(Pd nanostructure) electrodes (sample synthesized on 400 nm membrane during 350 s deposition period) recorded in 1 M $HClO_4$, potential scan from -0.2 to 0.7 V at 20 mV s^{-1} with 100 s sorption period at the initial potential E_s [V]: Plot A : -0.12 (1), -0.14 (2), -0.16 (3), -0.18 (4) and -0.20 (5) Plot B : -0.202 (6), -0.204 (7), -0.208 (8) and -0.21 (9); Plot C : -0.215 (10), -0.225 (11), -0.24 (12) and -0.28 (13)

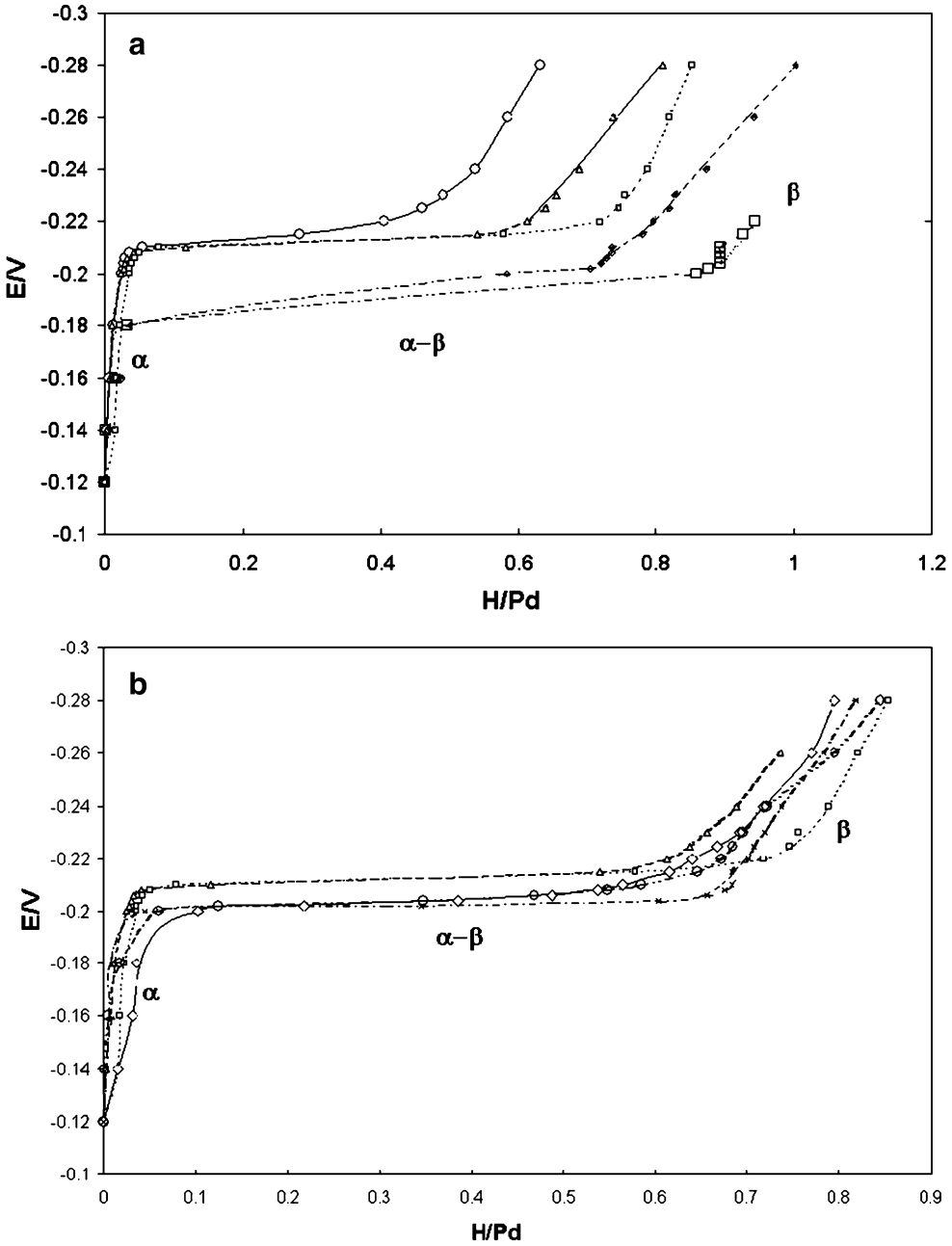

Fig. 4 Hydrogen absorption isotherms of the ITO\(Pd nanostructure) electrodes of various thickness: **Plot a** : samples: (○) 400 nm, 150 s; (△) 400 nm, 350 s; (□) 400 nm, 350 s; (x) 400 nm, 500 s; (□) 400 nm, 500 s; and obtained with membranes of various pore size: **Plot b**: samples: (△) 400 nm, 350 s; (□) 400 nm, 350 s; (◇)200 nm, 350 s; (○) 50 nm, 350 s; (x) 100 nm, 350 s

Hydrogen sorption

A representative selection of desorption curves is presented in Fig. 3. The most positive sorption potentials (E_s) value -0.12 V corresponds to the absence of hydrogen in palladium bulk. In this case peak at ~-0.03 V (Fig. 3, a, curve **1**) can be assigned to oxidation of adsorbed hydrogen. Similar behaviour is found for curves **2** and **3**, when curve **4** already demonstrates hydrogen absorption in the bulk leading to á palladium hydride formation.

The appearance of the second anodic peak at more negative potentials corresponds to hydrogen absorption in Pd bulk. This peak increases gradually as E_s becomes more and more negative (from-0.202 to-0.21 V, Fig. 3 b, curves **6–9**). For some samples the appearance of the α-phase can be noticed at already-0.14 →-0.16 V.

For even more negative E_s (from -0.215 to -0.28 V) (Fig. 3, c, curves **10–13**) the amount of hydrogen absorbed by Pd (the area under the desorption peak) increases rapidly evidencing the β-phase hydride formation. For some samples, the voltammograms corresponding to -0.28 V sorption potential (0.01 V RHE) exhibit the pronounced current shoulder at the very beginning of the anodic scan (Fig. 3, c). This hump is followed by a regular hydrogen

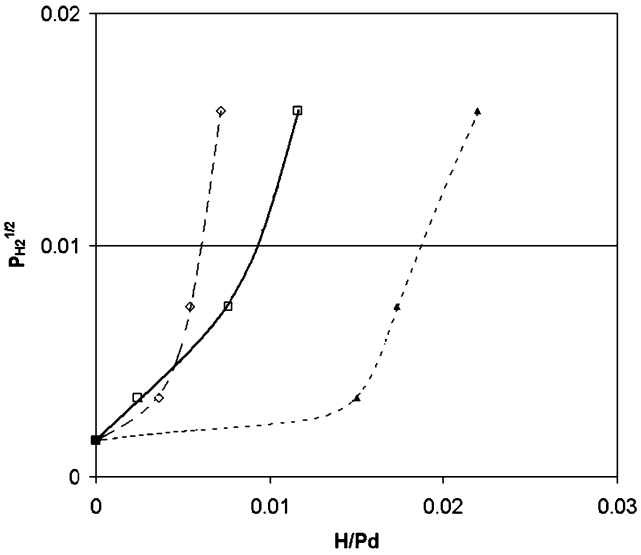

Fig. 5 The α-phase region plotted as Seaverts' isoterms for samples deposited on different membrane templates: (□) 400 nm, 350 s; (▲) 400 nm, 350 s; (◇) 100 nm, 350 s

desorption peak, a phenomenon observed earlier by other authors [13, 14]. We escape to assign this additional charge to β-phase hydrogen because it can result from oxidation of molecular hydrogen formed during the sorption period and dissolved in the near electrode layer of solution.

Figure 4a and b present hydrogen absorption isotherms constructed for the samples examined in this study. Figure 4a demonstrates the pronounced shift of the α-β transition plateau towards more positive values with the increase of deposition time (pressure). The plateau potential observed for the shortest 150 s time is close to 60 mV RHE, in agreement with the usual plateau position for less defective Pd materials. For longer deposition times this characteristic potential becomes essentially more positive (β-hydride formation is possible at lower hydrogen effective pressure). We assume that the defectiveness of more compressed Pd samples favours hydride formation. The length of the plateau also increases with deposition time (pressure), and the region of β-phase starts earlier for less compressed deposits. The lowest H/Pd ratio (below 0.7) and the shortest α-β transition region (c.a. 0.3 H/Pd) are observed for the shortest 150 s deposition time. Higher H/Pd values (around 0.9) and longer α-β plateaus (0.5 H/Pd) are found for 350 s deposition period. The highest H/Pd ratio (reaching 1.0) and the longest α-β transition regions (c.a. 0.8 H/Pd) are obtained for samples attained at 500 s deposition time. Only the former sample behaves like "usual" Pd [2]. Anomalously high amount of hydrogen in Pd lattice (>0.8) has been previously reported for Pd nanostructures obtained in different ways [3, 4, 6, 8–11, 19], but some of these effects could be mistakenly attributed to hydride formation, being in reality induced by the entrapment of H_2 in Pd defects.

Plot b in Fig. 4 illustrates the influence of membrane pore size (50 to 400 nm) for the samples obtained with the same deposition time (350 s). The effect on plateau potential is much weaker, and no evident correlation is found between H/Pd isotherms and the kind of membrane used for the sample synthesis. We suppose that the factors mentioned above like the length of plateau or the maximal amount of hydrogen sorbed in β-phase should somehow depend on palladium nanostucture. The highest value of H/Pd >1 was reported for Pd electrodeposit formed under simoultanious hydride formation [4]. This highly defective material can be considered as "self-compressed" by the grain boundaries in the course of initially formed hydride decomposition. Actually, in the previous studies of defective electrodeposited Pd (see discussion in [4]) correlation of excess hydrogen in α and β phases was always observed. This is however not the case for samples fabricated in membrane-separated cell.

For α-phase region (Fig. 5), we use the traditional Seaverts' plot $H/Pd \sim p_{H2}^{1/2}$, where P_{H2} is the effective hydrogen pressure as calculated from E_s using the Nernst equation. The limiting cases (the highest and the lowest H/Pd in α-phase) are presented. Typical H/Pd values are the same as for usual Pd electrodeposits which properties are varied by deposition potential [3]. Point defects are usually considered as hydrogen traps for excess hydrogen in α-phase. No indication of systematic effect of deposition conditions in membrane-separated cell on this type of traps is found.

Conclusions

Palladium deposits fabricated nanostructures using membrane separators are highly dispersed and tend to have anomalously high hydrogen sorption capacities. We relate these properties to mechanical pressure provided by compressed membrane. Taking into account that this pressure affects systematically β-phase properties and demonstrate no correlation with the α-phase behaviour, we assume that nanostructures contain the prolonged defective regions (consisting of at least several lattice units).

We assume at this stage that the membrane-induced pressure can affect the intergrain regions, by anology with the effect of much higher pressure used to prepare metallic compacts [20].

As usual the problem of electrodeposition in various nanostructured systems is to avoid formation of metal layer between current collector and structure forming component (a membrane or a 2D organic layer [21]). However our results point out that these less desirable layers of metal can demonstrate rather interesting properties and can be a subject to independent study.

References

1. Grier D, Ben-Jacob Z, Clarke R, Sander LM (1986) Phys Rev Lett 56:1264
2. Lewis FA (1967) The palladium-hydrogen system. Academic Press, London
3. Rusanova MYu, Grden M, Czerwinski A, Tsirlina GA, Petrii OA (2001) J Solid State Elecrochem 5:212
4. Petrii OA, Safonova TYa, Tsirlina GA, Rusanova MYu (2000) Electrochim Acta 45:4117
5. Natter H, Wettmann B, Heisel B, Hempelmann R (1997) J Alloys Comp 253:84
6. Rabinovich L, Lev O, Tsirlina GA (1999) J Electroanal Chem 466:45
7. Czerwiński A, Kiersztyn I, Grdeń M, Czapla J (1999) J Electroanal Chem 190:471
8. Tsirlina GA, Petrii OA, Safonova TYa, Papisov IM, Vassiliev SYu, Gabrielov AE (2002) Electrochim Acta 47:3749
9. Safonova TYa, Khaizallin DR, Tsirlina GA, Petrii OA, Vassiliev SYu (2005) Electrochim Acta 50:4752
10. Bartlett PN, Gollas B, Guerin S, Marwan J (2002) Phys Chem Chem Phys 4:3835
11. Rose A, Maniguer S, Mathew RJ, Slater C, Yao J, Russel AE (2003) Phys Chem Chem Phys 5:3220
12. Platt M, Dryfe AW, Roberts EP (2003) Electrochim Acta 48:3037
13. Berra D, Kuiry SC, Patil S, Seal S (2003) App Phys Lett 82:3089
14. Hwang PKR, Hwang YK, Kim MJ, Chang JS, Park SE (2004) J Coll and Interf Sci 276:333
15. Bartlett PN, Marwan J (2003) Chem Leter 15:2962
16. Bartlett PN, Marwan J (2004) Phys Chem Chem Phys 6:2895
17. Frydrychewicz A, Vassiliev SYu, Tsirlina GA, Jackowska K (2005) Electrochim Acta 50:1885
18. Masud A, Chudnovsky A (1999) Int J Plasc 15:1139
19. Cristina M, Oliviera F (2006) Electrochem Comm 8:647
20. Gleiter H (2000) Acta Materialia 48:29
21. Baunach T, Ivanova V, Kolb DM, Boyen HG, Ziemann P, Buttner M, Oelhafen P (2004) Adv Mater 16:2024